16th Australasian Fluid Mechanics Conference
Crown Plaza, Gold Coast, Australia
2-7 December 2007

Measurement of Free Stream Turbulence: It's Modeling and Computations

Tapan K. Sengupta, Pavankumar Mohanamuraly, Debopam Das and V. K. Suman

Department of Aerospace Engineering
Indian Institute of Technology Kanpur, KANPUR 208 016, INDIA

Abstract

Present research was initiated to study effects of free stream turbulence (FST) on flow instability and transition. Instabilities of some flows have been investigated qualitatively with respect to FST- but scant attention has been paid to compute extrinsic dynamics of flows due to FST. In actual flows, omnipresent background disturbances, e.g. FST triggers transition to turbulence. The motivation for the present work is to characterize and model FST, based on it's statistics, obtained from wind tunnel and flight test experiments. The developed model is applied to numerically study the receptivity of flow past circular cylinder to the FST.

Introduction Mueller et al [1] have studied the effect of free stream disturbance on low Reynolds number flow over an airfoil in the Reynolds number range of 100,000 to 1,000,000 and obtained the effect of FST on lift and drag. They report that at chord Reynolds number below 200,000 the boundary layer is extremely sensitive to FST and its effect depends on the magnitude, frequency content and sources of the disturbance. Both wind tunnel and free flight turbulence is characterized by the probability density functions (PDF) of the velocity time series that determine turbulence intensities and other higher order statistics [2]. In addition there are structural vibrations present in all wind tunnel data [1]. Similar vibrations of small amplitudes are expected to be present in flight data too.

So far, scant attention has been paid to compute extrinsic dynamics of flows due to FST, barring [3,4]. In [3], the effect was simulated as a stochastic laminar flow that at the inflow consists of uniform flow plus uniformly distributed random disturbances. In [4], a model for FST was developed, based on published wind-tunnel data to study chaotic-dynamics and intermittency of an aerofoil at high angles of attack. Such a model is appropriate for isotropic disturbance field.

Characterizing free stream turbulence (FST)
Wind tunnel and flight test data

Before we characterize FST, we note its importance from the results shown in figure 1, for flow past a circular cylinder at Re = 53, realized by considering two cylinders of diameters 5mm and 1.8mm placed in uniform flow, at speeds indicated in the figure. Despite the fact that the experiments were performed in the same tunnel, only at different speeds, cause the shedding pattern to be different from each other, and this signifies the importance of different background disturbance spectrum at different speeds.

In figure 2a, the measured wind-tunnel time series is shown without any model in the test section of a low speed tunnel with a test-section measuring 30cmX40cm and the contraction ratio of 9:1. The data was sampled at 10kHz over a period of 40sec, to avoid misrepresentation of higher order statistics.

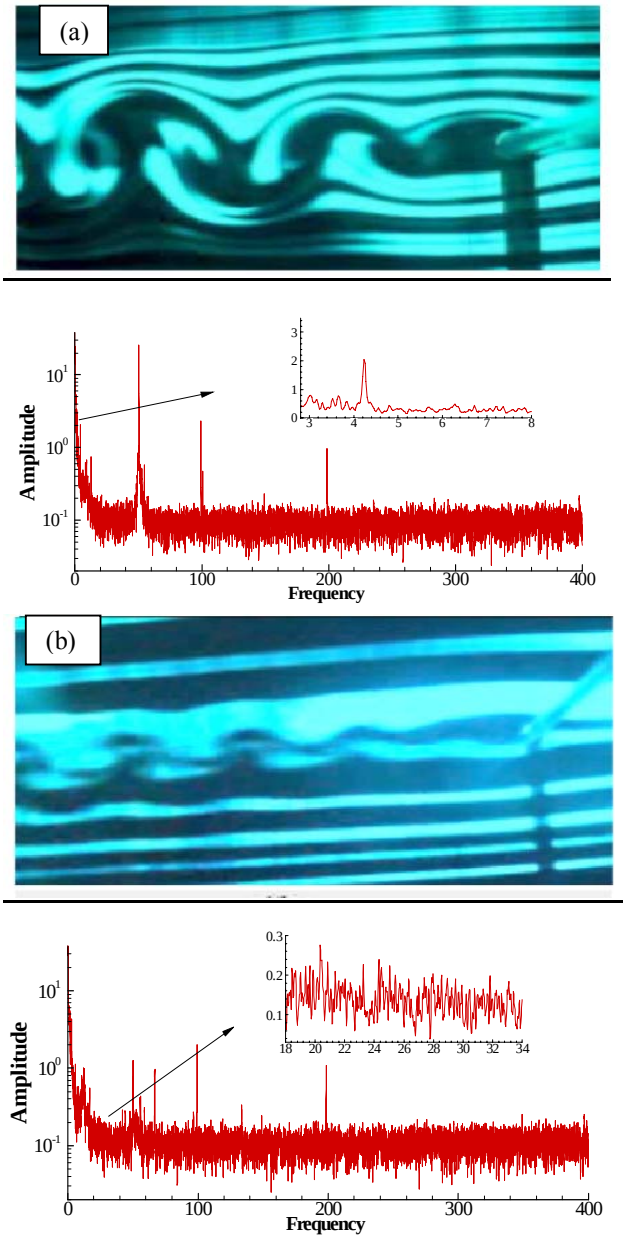

Figure 1: Experimentally observed flow for Re = 53 with (a) U = 17 cm/s, D = 5mm and (b) U = 46.9 cm/s, D = 1.8mm. FFT of empty-tunnel disturbance field is shown below the visualization picture at the same speed with the inserts showing amplitude near Strouhal frequency.

In figure 2a(ii), same data is shown with lower frequency components filtered out and it shows very high frequency fluctuations.

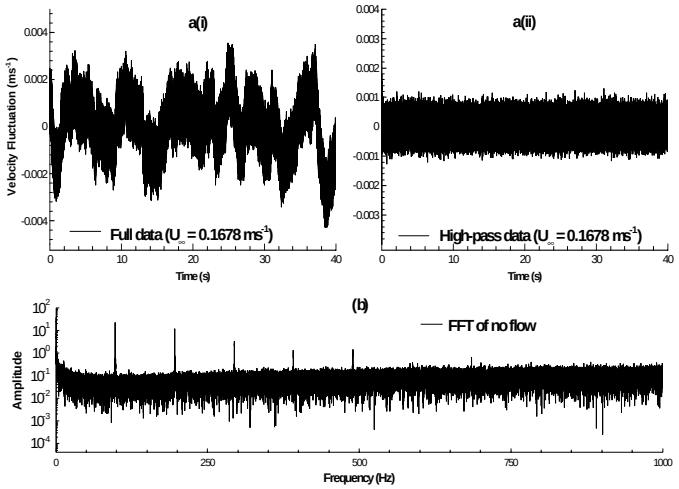

Figure 2 a. Time series of disturbance velocity (i) for full data and (ii) high-pass data. b. FFT of no-flow data (electronic noise).

The long tail of the fast Fourier transform (not shown) of the data in figure 2a(i), has contributions at high frequencies that is due to electronic noise, as evident from the FFT of no-flow data shown in figure 2b. Here, time series is represented by the probability density function (PDF) for the deviation from the mean, that is used to calculate all ordered statistics.

In figure 3, the time series and its PDF are shown for the data collected from flight tests, using the HANSA-3 aircraft of the Flight Laboratory, Aerospace Engg. Dept., IIT Kanpur, at the indicated altitudes.

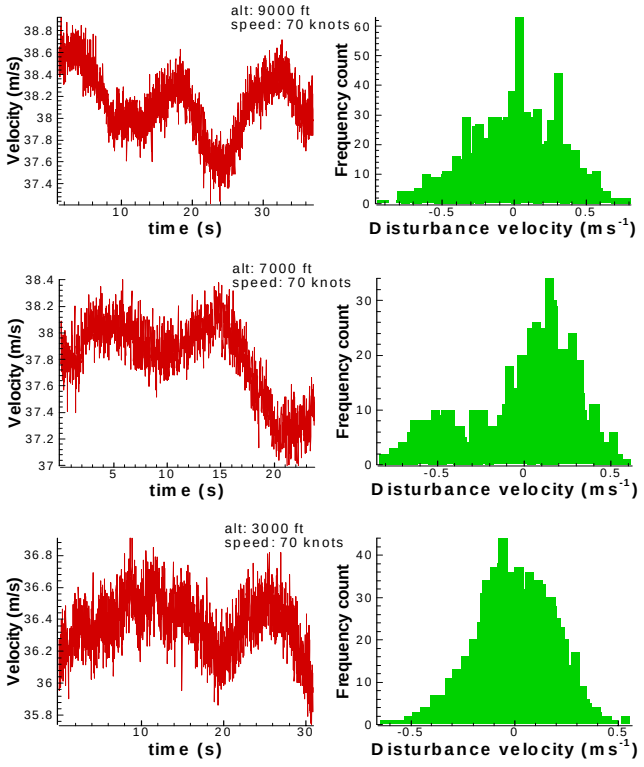

Figure 3 Time series of flight data (left) and it's histogram (right) at the indicated altitudes and speed.

Data is recorded with a Mini Air Data Boom of SpaceAge Control Inc. (model 100400), made of aluminium body with a stainless steel nose of 6.35mm diameter and 196.85mm length. The boom measured static and total pressures and direction of the boom axis with respect to flow axis with a flow angle sensor. Displayed time-series data on the left column of figure 3 are obtained for the mean wind speed of 36m/sec at the three altitudes of 2743.2m, 1828.8m and 914.4m. The corresponding PDFs are shown in the right column of figure 3. It is noted that the PDFs are not symmetric and significant number of events in the tail – implying the central role of higher order statistics of the associated FST measured by the time series.

Having obtained the time series for the background disturbance data from wind tunnel and flight data, their statistics are compared in figure 4 as a function of wind speed. We note that the fluctuating velocity component is only measured in the direction of the free stream. Thus, in figure 4(a), the displayed turbulent intensity (Tu) is taken as $Tu = \sqrt{u'^2}/U_\infty$. Thus, this is related to the standard deviation σ, of the fluctuation. The third and fourth moments are nondimensionalized by σ^3 and σ^4, respectively to obtain the skewness (Sk) and the kurtosis (Ku). In figure 4, the flight data are shown for the altitudes of 2.743km, 1.8288km and 0.9144km and the data show similar range for the respective quantities.

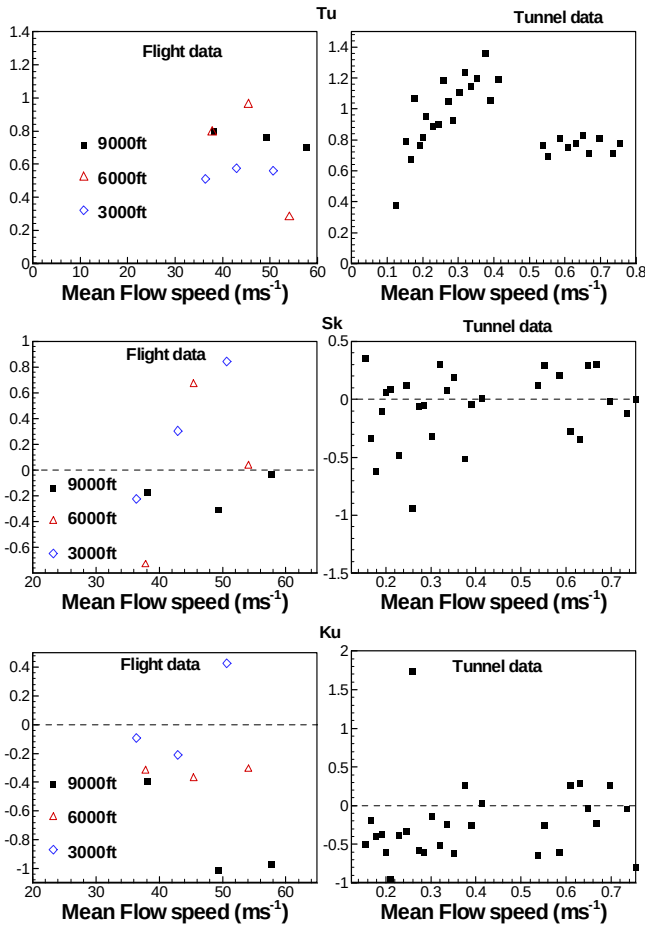

Figure 4 Comparison of turbulent intensity (top), skewness (middle) and kurtosis (bottom) of flight (left) and wind tunnel (right) data.

We note that for the wind tunnel, Tu changes discontinuously across 50cm/s wind speed. For lower speeds, the tunnel has

significant variations about the mean speed and it is evident from all the statistics shown here. While the wind tunnel displays maximum Tu of about 1.4% for a free stream speed of 40cm/s, for the flight data this is always below 0.9% . For higher flight altitudes, this progressively comes down. Similarly, skewness and kurtosis also reduces with altitude for the flight data, approaching the normal distribution. However, in the presence of unsteadiness (gust) of the free stream one would have significantly high skewness.

To assess the role of scalewise contribution to the various order moments of the FST in figure 5, we compare these three moments for the full with the high pass data. In figure 4, we have shown the skewness and kurtosis of the data, instead.

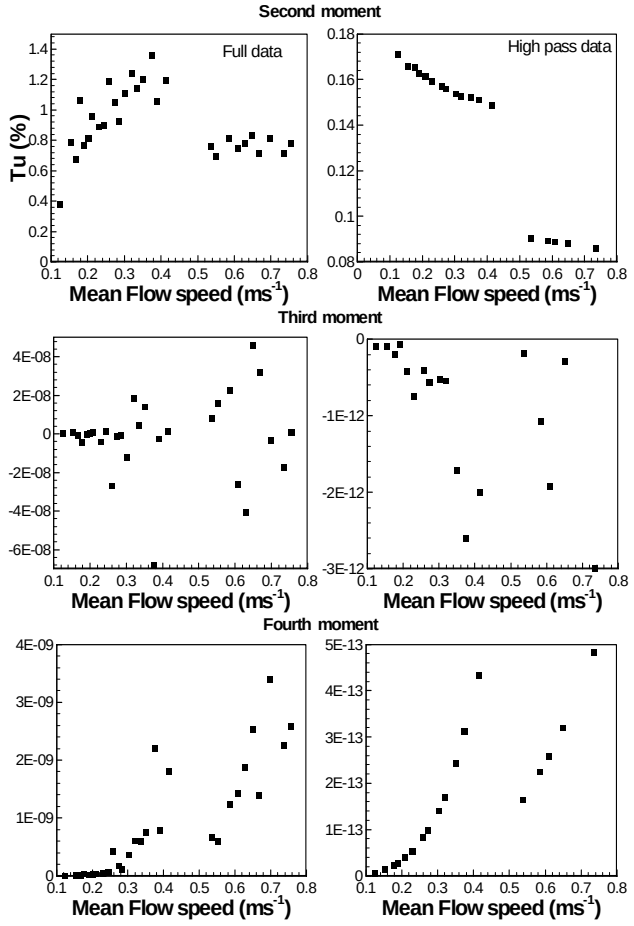

Figure 5 Contribution of high wave number components to second, third and fourth order moments of wind tunnel noise data.

It is noted that the moments for the full data appear without any pattern, while the high pass data shows definitive trend in its variation. For example, the high wave number contribution to turbulent intensity (*Tu*) of the empty tunnel is roughly about 10% of the total value and this shows plotted as a function of tunnel speed, in figure 5. The tunnel displays discontinuous *Tu* for flow speed exceeding 40cm/s. The third and fourth moments of the disturbance velocity with full- and high-pass data also show that the high wave number components to contributes a small fraction to the overall value, with discontinuous jump across 40cm/s speed. The high pass data show an increase in third and fourth moment to increase nonlinearly with speed up to 40cm/s and thereafter it falls suddenly, to increase further again from the low value with further increase in speed. This is a very specific feature of this tunnel. Also, it indicates the presence of significantly high unsteadiness of the tunnel speed at low frequencies, for lower speeds. This implies that the tunnel does not operate in a stable manner at speeds less than 40cm/s. However, in an experiment this large scale unsteadiness can manifest in exciting flow instabilities significantly. This will be studied here later. Figures 4 and 5 clearly show that all moments are dominated by large scale events, with the third moment or skewness playing a major role. It has been noted [5] that skewness of velocity signal indicates forward scatter via vortex stretching and for homogeneous turbulence it should be negative, if the time rate of change of enstrophy due to nonlinear interactions is positive.

Above mentioned unsteady nature of the oncoming flow in a wind tunnel at low speeds can also be seen from the histogram of the empty tunnel velocity data- as shown in figure 6 below. Bin counts at two velocities, in these figures, show multi-modal distribution. In [6], such multi-modal histogram has been identified with the effects of noise on the dynamics near bifurcation- an indication of evolving or time-varying flow (at low frequencies) inside the empty tunnel.

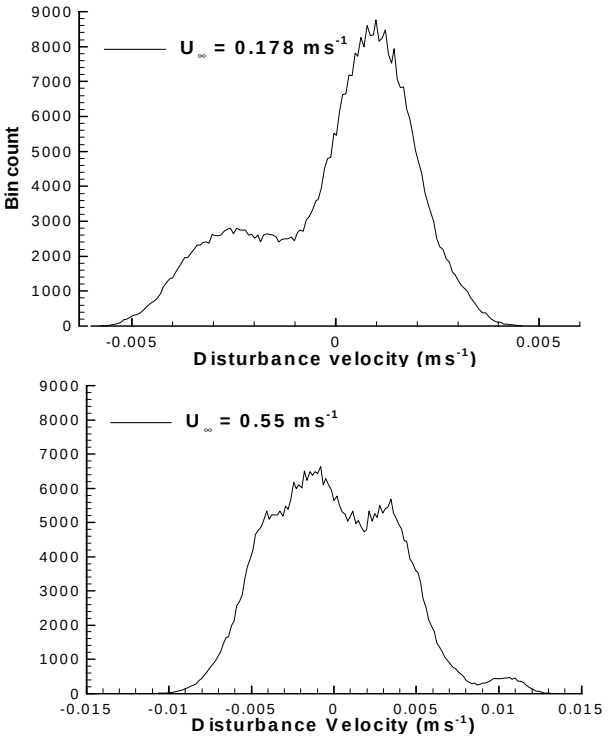

Figure 6 Histograms of disturbance velocities in the tunnel at the indicated speeds.

Modeling free stream turbulence

The discussions of the previous sections, indicate the need to model FST correctly, taking into account the presence of large-scale, low-frequency flow structures with the oncoming flow. A preliminary attempt was made in [4], where FST was modelled using a first order moving average model [7]. That model was proposed based on the observation in [8], that reported the histogram of a specific wind tunnel with an essentially symmetric PDF. As the skewness of such a histogram is zero, in the moving average model we fixed it's parameters, by matching the second and fourth moment of the histogram to that of the model. The simulation of Navier-Stokes equation with this FST

model is more realistic than solving any stochastic differential equation for a laminar flow [3].

Spark & Dutton [9] demonstrated a possible way of simulating turbulence using phase angles associated with the Fourier transform of a random time series. They considered an arbitrary random disturbance of Gaussian distribution. They obtained the Fourier transform and Fourier coefficients of the artificial Gaussian series and replaced the original spectrum with a -5/3 spectrum. They further assumed that the intermittent behaviour of FST is given by delta functions at discrete point of times and thus, constructed the phase angles of the new series with these coefficients. The reconstructed series represented qualitatively the nature of turbulence. Effort was made to incorporate the difference of random Gaussian noise and intermittent turbulence in the model. Similar model with uniformly distributed phase angles was used by Edwards [10] and Syono & Tanaka [11]. The main difference between the study of Spark & Dutton's with those reported in [10,11] is in the consideration of -5/3 spectra in the FST in [9].

Here, we propose an improvement on the model proposed in [4], by using the low frequency data of the FST as obtained experimentally. In this modified model, we represent the streamwise disturbance component of velocity field by,

$$u' = e_t + \alpha e_{t-1} + \sum_{j=1}^{N} a_j e^{ik_j(x-ct)} \qquad (1)$$

where the first two terms are given by Gaussian distribution at successive time steps with unknown standard deviation (σ), and the last term represents the low frequency component of noise (as shown in figure 2) that is facility- and speed- dependent; c is the phase speed of propagation of these coherent structures. When we use such model at the inflow of a computational domain, while solving Navier-Stokes equation – the exact value of c is not very important.

In the FST model, the large-scale anisotropy of the oncoming flow is retained up to a low frequency range, as in the FFT of the empty tunnel record at the same speed. These would account for the skewness of the data shown in figure 4. The moving average time series of order one [7], is used to obtain the Gaussian distribution in equation (1), whose second and fourth moments are fixed in such a way that the composite signal's moments match with the high-pass experimental time series. This way one constructs a FST model corresponding to the actual flow in the experiment. In figure 7, FFT of the experimental wind-tunnel data for the disturbance velocity is compared to the synthetically generated FST model of equation (1), for the mean flow speed of 17cm/s. It is evident fro this figure that the major peaks of the FFT of the actual data is retained in the synthetic FST model, all the way up to frequency range of 200 Hz. This is done purposely, as we have used the FST model for computing flow past a circular cylinder. The essential aim is to retain the FST signature up to and above the Strouhal number of Karman vortex shedding (KVS). In performing this exercise, we note that the KVS is related to an instability of the wake bubbles that causes shedding of them alternately. This is usually simulated without the need for any background excitation. That is, the numerical errors associated with truncation and round-off is sufficient to initiate this instability. However, in a noisy flow with FST, the system dynamics can be significantly altered by the constant excitation at many frequencies simultaneously with finite amplitude. In such a case, the evolving wake bubbles can suffer Kelvin-Helmholtz instability. This is investigated next.

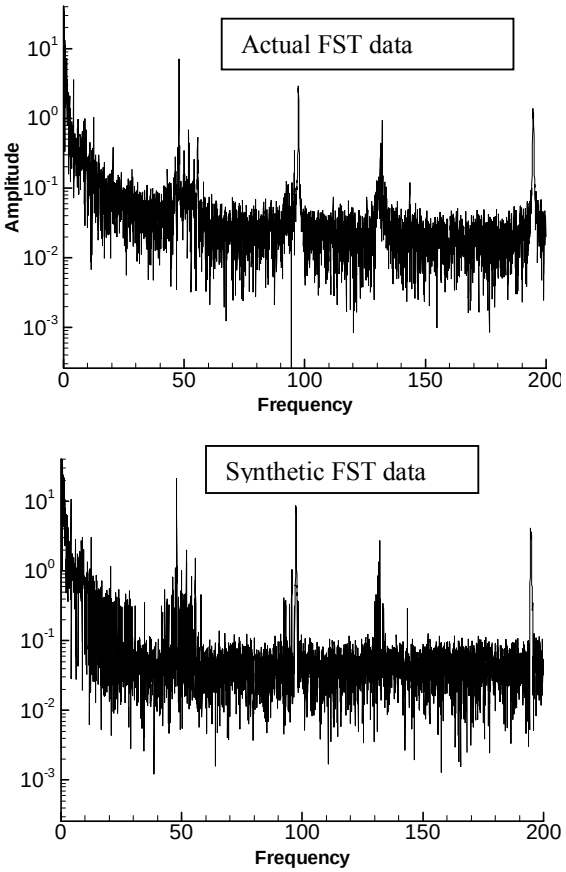

Figure 7 Actual and modelled FST data using equation (1).

Computing flow past cylinder in the presence of FST

The flow past a circular cylinder is simulated here for trans-critical Reynolds numbers- that has often shown sensitive dependence on background disturbances. We specifically note the experiments of Homann [12], where the flow was created in a highly viscous fluid and the author reported no shedding of vortices below Re = 65. Otherwise, from different experiments performed in different facilities, one notes critical Reynolds numbers varying from 40 to 53 [13-15]. This is significantly different from the value reported in theoretical studies that identify criticality with Hopf bifurcation [16,17].

The formulation, numerical method employed in the present simulation is the same that is reported in [18]. Here, the two-dimensional Navier-Stokes equation is solved in the streamfunction- vorticity formulation in a polar domain with the outer boundary placed at twenty diameter distance from the centre of the cylinder. The nonlinear convection terms in the vorticity transport equation is discretized using a high accuracy compact scheme and the time marching is performed using four-stage Runge- Kutta method.

In figure 8, computational flow with the FST model, for *Re* =55, is compared with the experimental results of [12]. The experimental results [12] in figure 8(a), show the absence of shedding with the near-wake symmetric, while some undulations noted in the far wake. For the FST model, we have prescribed Tu = 0.001 with the oncoming flow at the inlet of the computational domain. With the FST model switched-on with a small value of *Tu*, the computed results match with the experiments in most details- the undulation of the far-wake is related to pulsation of the near-wake bubbles caused by the imposed noise.

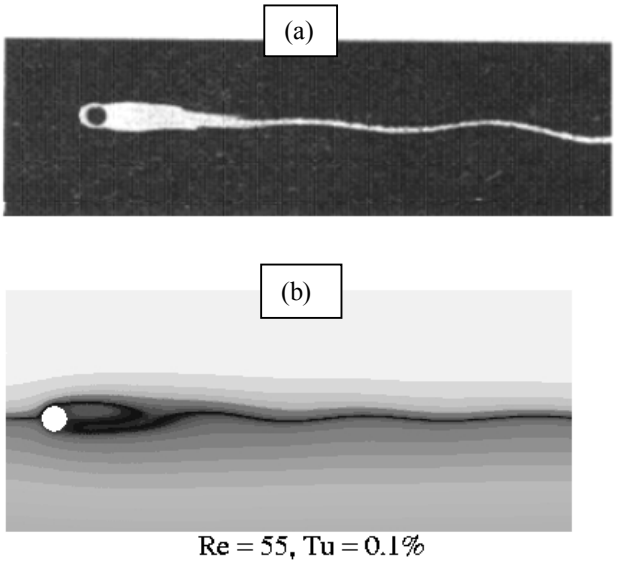

Figure 8 (a) Experimental results due to Homann [12] for Re = 55 obtained in an oil-tunnel, (b) Present computed result with the FST model as given by equation (1) with turbulent intensity, Tu, = 0.1%.

The events seen in figure 8, shows an undulating wake without the alternately shed vortices from the cylinder wall- as is usually the case for KVS. Instead, the primary wake-bubble is seen continuously in the near wake and the limiting streamline constituting the edge of the recirculating bubble is a seat of thin vortex sheet, that is excited by the FST via the Kelvin-Helmholtz instability (KHI) mechanism. This causes the sheet to undulate and a small quantity of vorticity is released in the wake. This will also show up as unsteadiness in any measured signal in the wake. It is also expected that the events would occur at a higher frequency.

To understand the role of disturbance in causing KVS and KHI, another case is computed for Re = 53, exposed to higher level of FST. These results are shown in figure 9 below.

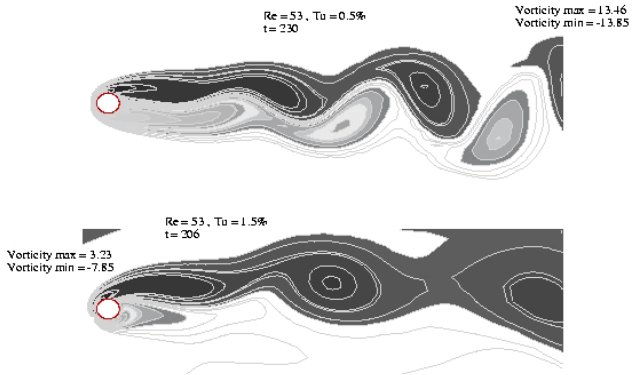

Figure 9 Computational vorticity contours for Re = 53 case with Tu = 0.5% (top) and Tu = 1.5% (bottom). Maximum and minimum values of vorticity are also marked for both the cases.

In figure 9, the computed vorticity contours are shown plotted for the cases with Tu = 0.5% (top) and 1.5% (bottom), respectively. For the displayed cases, the maximum and minimum values of vorticity are marked in the frames. It is interesting to note that for the lower FST case, the maximum and minimum values are almost same, implying the near symmetry of the vorticity field, although there is asymmetry in the far-wake, as the formation length is significantly high. Also, we note that the vorticity values are twice for the lower Tu case, as compared to the higher Tu case. This is also due to the symmetry of the bubble and the larger formation length, that allow vorticity evolution to higher values, due to lower impetus created by lower FST. In contrast, for the higher FST case, the turnover time for each cycle is shorter, due to larger amplitude of excitation field that causes the loss of symmetry earlier. For both the cases, the synthetic FST is created while matching the Tu value. For the lower FST case, the solution is shown for t = 230, at a time where one can notice alternately shed vortices. This is similar to the case shown in figure 8, where none of the wake-bubble was detached completely at any time and only weak vortices were shed from the tip of the attached primary wake. However, the strength of FST is five times higher and the stripped vortices are of larger dimension, even though their strength is significantly lower. The displayed solution for the higher FST case is at t = 203.

The above description of the flow field can also be seen in the time history of the lift experienced by the cylinder in each case, that is shown below in figure 10. The lift and drag (not shown here) values are calculated from the calculated vorticity field by solving the vorticity transport equation and the pressure field obtained by solving the pressure Poisson equation for the total pressure- a description of the equation and solution method is also given in [18]. The latter is required for the correct evaluation of the total pressure field – that being a good measure of mechanical energy of the flow. The calculated total pressure reduces to the static pressure on the no-slip surface of the cylinder, that allows calculating it's contribution to lift and drag coefficients.

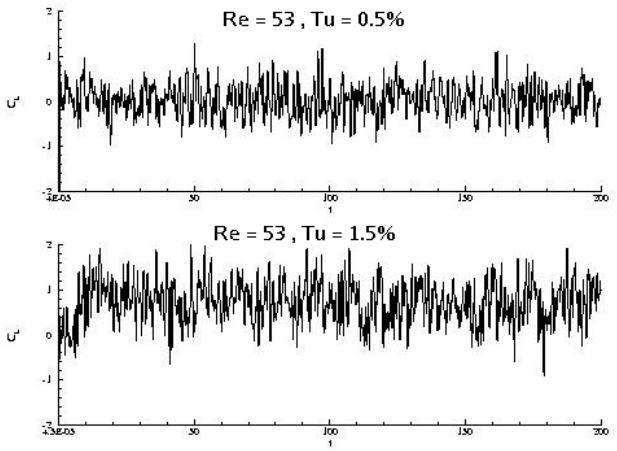

Figure 10 Time-variation of lift coefficients for the computed cases shown in figure 9.

Interestingly, the displayed lift variation does not immediately display any preferred time scale or frequency – as the absence of any apparent periodicity in the time series. Also, it is noted that the time average of lift is quite different for these two cases. This is due to the different mechanism of vorticity dynamics in each case- as discussed above with respect to figure 9 results. While the seemingly absent time scale(s) can be seen if we perform a Fourier transform of the lift time series shown in figure 10. This is shown next in figure 11.

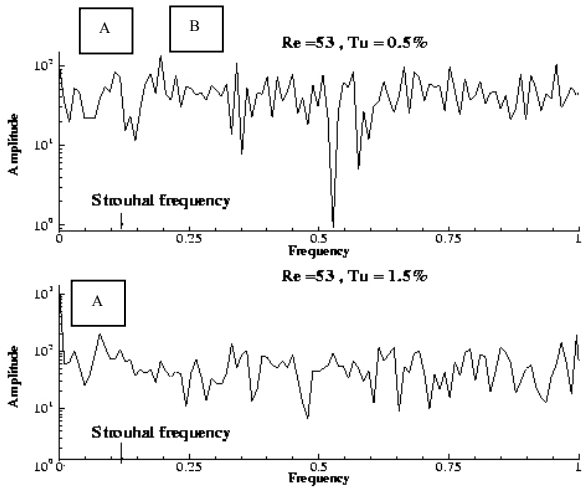

Figure 11. Fourier transform of the lift data shown in figure 10. The Strouhal frequency is marked for reference by a vertical arrow-head, in both the figures.

In the figure, the Fourier amplitude is plotted in the log-scale against a non-dimensional frequency. For the case of Re =53, one notes the Strouhal frequency, by a vertical arrow-head. This is at a value given by, St = 0.12. For the lower FST case, we note two peaks, marked as A and B, with the latter having a larger amplitude. The lower peak is very close, but at a lower value, as compared to the Strouhal number. This slight de-tuning is due to the presence of noise – a typical feature of non-linear systems, see e.g [6] and other references contained therein. Even for the higher FST level case also, one notices the most significant peak at A that is also lower than the Strouhal number. This frequency is slightly lower than that for the lower FST case – showing that the detuning to increase with the amplitude of the noise.

The presence of the second peak, for the lower FST case, at B has higher amplitude, as compared to the amplitude at A. These events at a higher frequency are caused by the stripping of vortices from the wake-bubble by the lower FST, that tries to destabilize the equilibrium symmetric wake-bubble configuration. But that is not strong enough to completely dislodge any one of the wake bubbles completely. This stripping process occurs at a faster pace, as compared to the overall shedding of larger vortices alternately in the wake. When the FST level is increased to Tu = 1.5%, the symmetric wake-bubble configuration is destabilized, that causes vortices to be shed at a faster rate from the near vicinity of the cylinder.

Conclusions

Present interest in studying the effects of free stream turbulence on flow instability and transition is pursued here as a set of multiple activities. In general, instabilities of some flows have been investigated qualitatively with respect to FST- but little attention has been paid to compute extrinsic dynamics of flows due to FST- except in [3,4]. The need for this approach is established via the results of figure 1, where the same Reynolds number flow is established in the same wind-tunnel by choosing two different diameter cylinder kept at two different free stream speed. This shows the shedding patterns to be different, implying the central role of background disturbances in the two cases.

As compared to solving the problem as a stochastic laminar flow in [3], the present approach is an improvement of the method adopted in [4], where the extrinsic dynamics of the flow is calculated with respect to the actual FST as measured from wind-tunnel and flight experiments using an aircraft at different altitudes. In the first part of the work, we characterize background noise data collected from these two sources, in terms of their statistics, up to the fourth order. Presented data in figures 2 to 6, show similarity in pattern of wind-tunnel noise statistics with the data from the flight experiments. We specifically note the role of low frequency noise that shows up as different skewness of the data. We essentially follow the model of [4], by matching the second and fourth order statistics of the actual data in constructing a synthetic time series using the moving average method of order one [7] and to this we add the FFT of the actual wind-tunnel data to simulate the skewness of the background noise. The result is the match of the synthetic FST model with the actual FST data- as shown in figure 7. This is the second phase of the reported work.

In the final part of the work, we use the developed model for calculating flow past a circular cylinder and compare it with experimental results of [12] – as shown in figure 8. It appears that the visualized flow of [12] at Re = 55 can be computed as a flow experiencing very low FST of Tu = 0.1%. Extrinsic non-linear dynamics of the flow is studied further for Re =53, by considering two FST levels of Tu = 0.5% and 1.5%. Various results are shown in figures 9 to 11, that brings out the characteristics of such flows. We establish the role of Kelvin-Helmholtz instability at lower FST level, that shows the presence of two peaks for the lower FST case. One corresponds to alternate vortex shedding at a lower frequency, and the other occurring at higher frequency is due to Kelvin-Helmholtz instability. For larger FST level, this latter events do not occur and one sees a predominant peak near the Strouhal number. We also notice detuning of the predominant frequency from the Strouhal number due to non-linearity. This establishes the need to study these problems as one of receptivity to FST.

Acknowledgments

The authors acknowledge the scientific and technical staffs of the Flight Laboratory, Dept. of Aerospace Engineering, IIT Kanpur in procuring and pre-processing all the flight data reported in this paper.

References

[1] Mueller, T.J., Pohlen, L.J., Cnigliaro, P.E. & Jansen Jr., B.J., The influence of free-stream disturbances on low Reynolds number airfoil experiments, *Expts. in Fluids.*,**1**, 1983, 3-14.

[2] Pope, S.B., *Turbulent Flows*, Cambridge Univ. Press, Cambridge, U.K. 2000.

[3] Lucor, D. & Karniadakis, G.E., Noisy inflows cause a shedding-mode switching in flow past an oscillating cylinder, *Phys. Rev. Letters,* **92**, 2004, 154501-1 154501-4.

[4] Sengupta, T.K., De, S. & Gupta, K. Effect of free-stream turbulence on flow over aerofoil section at high incidence, *J. Fluids & Struct.*, **15**, 2001, 671-690.

[5] Batchelor, G.K. & Townsend, A. A., Decay of vorticity in isotropic turbulence, *Proc. Roy. Soc. (London) A*, **191**, 1947, 534-550.

[6] Juel, A., Derbyshire, A.G. & Mullin, T., The effect of noise on pitchfork and Hopf bifurcations, *Proc. Roy. Soc. (London) A*, **453**, 1997, 2627-2647.

[7] Fuller, W.A., *Introduction to Statistical Time Series*, Wiley, New York, 1978.

[8] Frisch, U. *Turbulence,* Cambridge Univ. Press, Cambridge, U.K., 1995.

[9] Spark, E.H. & Dutton, J.A., Phase angle considerations in the modeling of intermittent turbulence, *J. Atmosph. Sc.* **29**, 1972, 300-303.

[10] Edwards, S.F., The statistical dynamics of homogeneous turbulence, *J. Fluid Mech.*, **18**, 1964, 239-273.

[11] Syono, S. & Tanaka, H., On frequency distribution of wind speed and direction in turbulent flow, *J. Meteor. Soc. Japan*, **44**, 1966, 89-100.
[12] Homann, F., Einfluss groesser zaehigkeit bei stroemung um zylinder, *Forschung auf dem Gebiete des Ingenieurwesens,* **7(1)**, 1936, 1-10.
[13] Kovasznay, L.S.G., Hot-wire investigation of the wake behind cylinders at low Reynolds numbers, *Proc. Roy. Soc. London A*, **198**, 1949, 174-190.
[14] Roshko, A., On the drag and shedding frequency of two-dimensional bluff bodies, *NACA TN,* **3169**, 1954.
[15] Kiya, M., Suzuki, Y., Mikio, A. & Hagino, M., A contribution to the free stream turbulence effect on the flow past a circular cylinder, *J. Fluid Mech.*, **115**, 1982, 151-164.
[16] Zebib,A, Stability of viscous flow past a circular cylinder, *J. Eng. Math.,* **21**, 1987, 155-165.
[17] Morzynski, M. & Thiele, F., Numerical investigation of wake instabilities, In *Bluff-body Wakes, Dynamics and Instabiilties (eds. Eckelmann, Graham, Huerre & Monkewitz),* Springer Verlag, Berlin, 1993.
[18] Dipankar, A., Sengupta, T.K. & Talla, S.B., Suppression of vortex shedding behind a circular cylinder by another control cylinder at low Reynolds numbers, *J. Fluid Mech.*, **573**, 2007, 171-190.